Synthesis and Characterization of an Acrylate-Copolymer-Based Antistatic Agent Composed of a Single-Ion Conductive Polymer Electrolyte

Dongyang Guo, Jiliang Wang, Jingxin Lei

State Key Laboratory of Polymer Materials Engineering, Polymer Research Institute, Sichuan University, Chengdu, China 610065

Received 27 December 2009; accepted 23 May 2010
DOI 10.1002/app.32849
Published online 9 September 2010 in Wiley Online Library (wileyonlinelibrarycom).

ABSTRACT: Monomethoxy poly(ethylene glycol) acrylate (MPEGA) was synthesized through the esterification reaction of acrylic acid and methoxy poly(ethylene glycol)s (MPEGs) of different molecular weights. Then, MPEGA was copolymerized with methyl methacrylate, butyl acrylate, and β-carboxyethyl acrylate neutralized with potassium hydroxide via conventional solution polymerization. In this way, a single-ion conductive polymer-electrolyte-based antistatic agent (PEAA), in which potassium (K) ions were used as charge carriers, was obtained. The molecular structure, coordination effects between ether oxygen (EO) groups and K cations, ionic conductivity, and crystallization ability of the copolymer were characterized with Fourier transform infrared, conductivity measurements, polarizing optical microscopy, and differential scanning calorimetry, respectively. The crystallinity of the synthesized PEAA apparently decreased with the molecular weight of MPEG and the EO/K molar ratio decreasing, and this led to a corresponding enhancement of the conductivity. The dependence of the conductivity of the copolymer on temperature could be divided into different linear parts, and each was in good agreement with the Arrhenius equation. Moreover, the dependence of the conductivity on the relative humidity (RH) revealed that the PEAA could maintain high ionic conductivity ($\sim 10^{-6}$ S/cm) even at the low RH of 10%. This implies the potential widespread application of PEAAs for the preparation of antistatic composites and especially poly(vinyl chloride)- and poly(methyl methacrylate)-related composites because of their considerable miscibility. J Appl Polym Sci 119: 2674–2682, 2011

Key words: copolymerization; morphology; polyelectrolytes

INTRODUCTION

To reduce the surface or volume resistivity and dissipate the high electric charge density on the surfaces of common plastics for which the surface resistivity ranges from 10^{14} to 10^{18} Ω/sq, both antistatic agents (including ionic and nonionic surfactants) and conductive fillers (e.g., carbon blacks and metal fibers) are commonly used.[1–5] Unfortunately, antistatic agents cannot endow polymers with a persistent antistatic ability. Moreover, the surface resistivity of polymers is strongly dependent on the relative humidity (RH) of the ambient environment, and this further limits widespread applications in some special fields. Currently used conductive fillers suffer the problems of relatively high cost and filler migration or metal decay in the polymer matrix and on the surface; this also restricts their large-scale applications in industry.[6]

Solid polymer electrolytes (SPEs), because of their capacity for ionic conductivity, have received considerable attention for the development of high-energy-density, leak-proof batteries during the last 2 decades.[7–10] Generally, the reported SPEs suffer the main problems of low conductivity and bad mechanical properties when they are applied in rechargeable cells. However, the use of ion-conductive SPEs as antistatic agents to impart an antistatic capacity to an insulating polymer is a novel development that takes into account both the permanent ion conductivity and the light color or dyeing properties of SPE-based antistatic agents as long as their dispersion in the polymeric host and the thermoprocessing ability can be properly handled. Recently, many relevant works regarding bi-ion, SPE-based antistatic composites have been finished in our laboratory.[11–15] However, to the best of our knowledge, there have been no previous reports regarding the use of single-ion SPEs as RH-insensitive antistatic agents.

In this work, we synthesized a single-ion, SPE-based polymeric antistatic agent based on acrylate copolymers in which the oligo-ether groups and

Correspondence to: J. Lei (jxlei@scu.edu.cn).

potassium (K) cations played the roles of ligands and carriers, respectively; we considered its high conductivity, low price, and easy preparation. The effects of the molecular weight (MW) of methoxy poly(ethylene glycol) (MPEG) and the concentration of K on the conductivity at different temperatures and RHs were investigated. The prepared antistatic agent was also characterized with Fourier transform infrared (FTIR), conductivity measurements, polarizing optical microscopy (POM), and differential scanning calorimetry (DSC). The single-ion polymeric antistatic agent showed potential for poly(vinyl chloride) (PVC) and poly(methyl methacrylate) (PMMA) antistatic composites; this was attributed to its permanent ion conductivity even at low RHs and its good compatibility with the polymeric host. Furthermore, the electrostatic discharge (ESD), thermoprocessing, and mechanical properties of corresponding PVC composites were also evaluated recently, but they will be reported later to keep this article simple.

EXPERIMENTAL

Materials

Acrylic acid (AA; analytical grade; Kelong Chemical Reagent Co., Chengdu, China) and methyl methacrylate (MMA; analytical grade; Kelong Chemical Reagent) were distilled under reduced pressure and stored in a refrigerator. MPEG, purchased from Changxing Chemical Reagent Co. (Guangdong, China), was dried *in vacuo* at 80°C overnight before use. β-Carboxyethyl acrylate (β-CEA) was also supplied by Changxing Chemical Reagent and was used without further purification. All the other chemicals used in this experiment were analytically pure.

Synthesis of the polymer-electrolyte-based antistatic agents (PEAAs)

PEAAs were obtained with the following steps. First, stoichiometric AA, MPEGs with MWs of 200, 400, 600, 800, and 1000, a catalyst, and toluene were added to a three-necked flask equipped with a water segregator. Then, the temperature of 120°C was used for the esterification reaction of monomethoxy poly-(ethylene glycol) acrylate (MPEGA). The reaction was stopped when theoretically stoichiometric water was obtained from the water segregator. Toluene and unreacted AA were distilled under reduced pressure. The resulting mixture was washed with petroleum ether several times and then dried in a vacuum oven at 50°C for 24 h. The synthesized MPEGA derived from MPEG 600 was named MPEGA6. The resulting MPEGAs with different MWs were copolymerized with set concentrations of MMA, butyl acrylate (BA), and β-CEA neutralized with potassium hydroxide

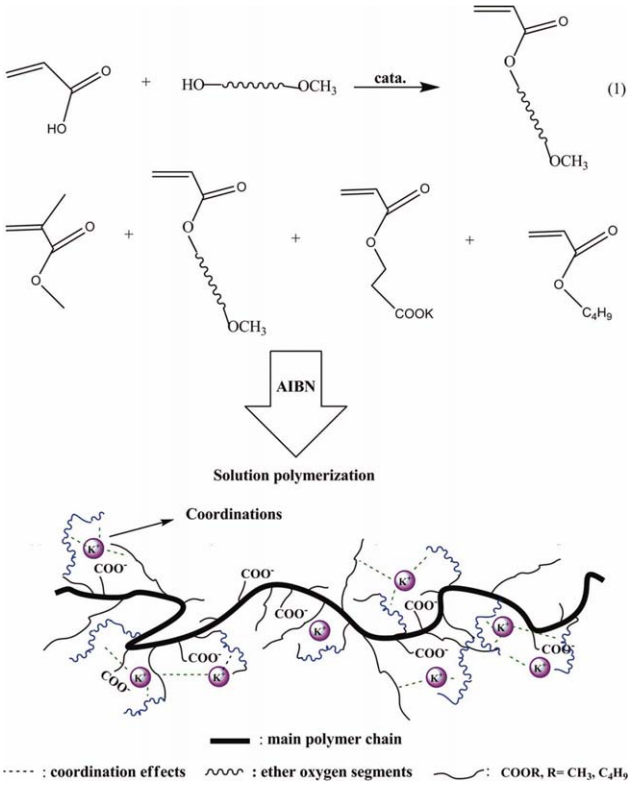

Scheme 1 Schematic of the synthesis route of the PEAAs. [Color figure can be viewed in the online issue, which is available at wileyonlinelibrary.com.]

(KOH) by solution polymerization; ethylacetate was used as the solvent. The content of the solid polymer was designed to be 40 wt %. After polymerization, the products were poured into petroleum ether and then precipitated into hexane several times. The precipitates were dried *in vacuo* at 50°C for 48 h. The synthesis route for the PEAAs is shown in Scheme 1. PEAAs originating from MPEG 200 with ether oxygen (EO)/K molar ratios of 6/1, 8/1, and 10/1 were named S2-6, S2-8, and S2-10, respectively. Other PEAA specimens were defined in the same way; for example, S6-6 represents the PEAA sample derived from MPEG 600 with the EO/K molar ratio of 6/1.

Characterization

FTIR measurement

Samples were cast onto a spectrograde KBr substrate for the FTIR study. Infrared spectra were obtained with an FTIR spectrophotometer (Nicolet 560, Thermo Nicolet Corp., Grove, United States) and recorded via the averaging of 64 scans with a wavenumber resolution of 4 cm^{-1}.

Conductivity measurement

The volume resistivity of PEAA samples with dimensions of 25 mm × 10 mm × 5 mm were

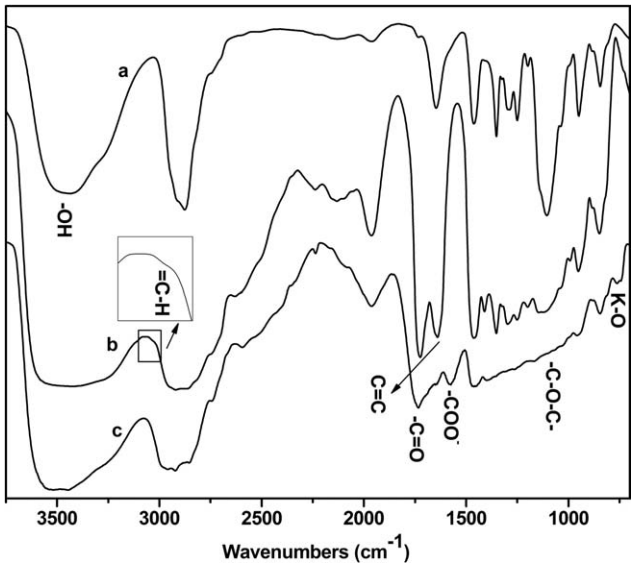

Figure 1 FTIR spectra of (a) MPEG, (b) MPEGA, and (c) S6-6.

measured with a digital volume resistivity meter (UT50/UT101, You Li De Corp., Guangdong, China) at different RHs in an N_2-flow-permitting glove box in which the RH and temperature of the system were controllable. It was also measured from 30 to 90°C at a low RH of 12% with the same instrument. The conductivity was then calculated as follows:

$$\text{Conductivity} = L/R_V S$$

where L, R_V, and S are the thickness of the sample, the volume resistivity of the sample, and the area of the electrode, respectively.

POM analysis

For microscopy observations, a POM instrument (XSZ-H, Guangdian Instrument Co., Chongqing, China) equipped with a digital camera (Nikon Coolpix P6000, Nikon Corp., Tokyo, Japan) was used in the ambient environment. The image magnification was 400×.

DSC analysis

DSC of PEAAs was carried out with a DSC204 analyzer (Netzsch, Selb, Germany) at a heating rate of 10°C/min in the temperature range of −100 to 80°C under a nitrogen atmosphere.

RESULTS AND DISCUSSION

FTIR results

The esterification reaction and solution polymerization were confirmed by the FTIR spectra illustrated in Figure 1(a) for MPEG 600 and in Figure 1(b,c) for the synthesized MPEGA6 and S6-6, respectively. The characteristic vibration bands at approximately 3450 cm^{-1} for the —OH groups and at 1050–1105 cm^{-1} for the —C—O—C— groups can be observed in Figure 1(a). Moreover, the peaks at 2950–2850 cm^{-1} correspond to the —CH_2 and —CH_3 stretching of MPEG. After the esterification reaction between AA and MPEG, new vibration bands at 3000 and 1640 cm^{-1} for the C=C groups and at 1730 and 1140 cm^{-1} for the —C=O and —C—O—C— groups could be seen [Fig. 1(b)]; they indicated that MPEGA was successfully synthesized by this method. As shown in Figure 1(c), after copolymerization with MMA, BA, and β-CEA neutralized with KOH, the vibration bands at 3000 and 1640 cm^{-1}, assigned to the C=C groups, disappeared. Meanwhile, absorption bands at 1570 and 760 cm^{-1}, assigned to the —COO^- and K—O groups, were detected, and this implied that the target single-ion polymeric antistatic agents were successfully synthesized.

It has been proved that FTIR analysis is a useful method for investigating the interactions between polymeric molecular chains with EO groups and alkali salts.[16–19] Partially enlarged views of the vibration bands of the —C—O—C— groups of S6-*X* (*X* = 6, 8, or 10) and S*Y*-6 (*Y* = 2, 6, or 10) are shown in Figures 2 and 3, respectively. A visible characteristic vibration of the —C—O—C— groups was detected for S6-10; however, it was invisible for S6-6 (Fig. 2). With the K concentration increasing (EO/K ratio = 10/1–6/1), the characteristic peaks of —C—O—C— at 1150 and 1050 cm^{-1} broadened, and this implied that the dissociation effect of K became stronger[20] (i.e., an increase in the carrier density). As shown in Figure 3, the characteristic vibration of the —C—O—C— groups was apparently detected for

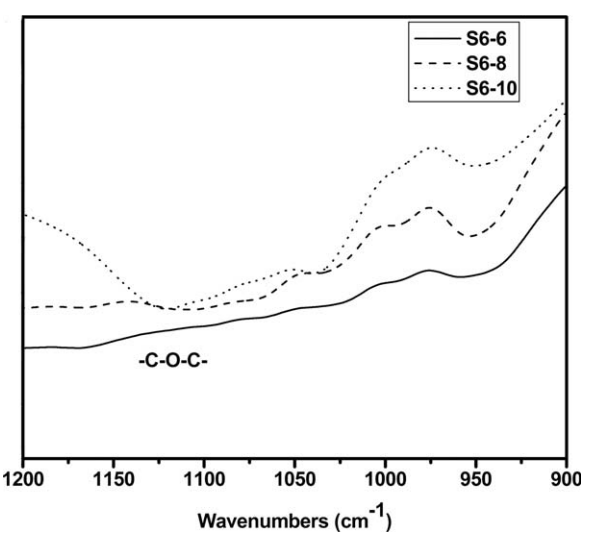

Figure 2 FTIR spectra of S6-*X* (*X* = 6, 8, or 10).

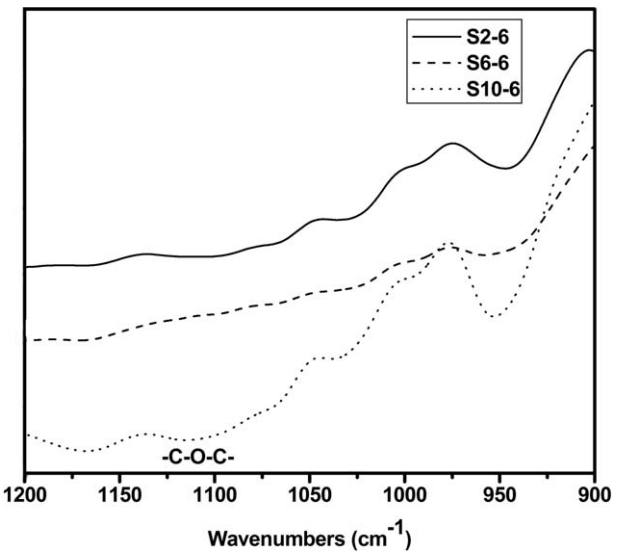

Figure 3 FTIR spectra of SY-6 ($Y = 2$, 6, or 10).

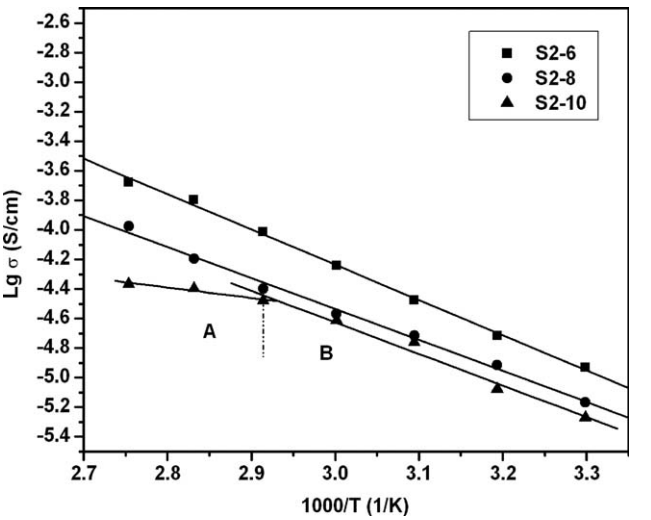

Figure 4 Dependence of the conductivity (σ) of S2-*X* ($X = 6$, 8, or 10) on temperature (T).

S10-6; however, it almost disappeared for S2-6 and S6-6, and this indicated that K preferentially coordinated with oxygen atoms of EO groups of PEAAs with a low-MW MPEG at the same salt concentration.

Conductivity measurement

The impact of the temperature on the conductivity of different PEAAs is shown in Figures 4–8. The experimental data indicated that the conductivity of PEAAs increased from 10^{-6} to 10^{-4} S/cm when the temperature increased from 30 to 90°C; this was attributed to the fact that the increase in the temperature enhanced the mobility of the polymer chains simultaneously, and this was favorable for the migration of K. Moreover, the number of charge carriers also increased with the temperature because of the rise of the dissociation of coordinated K. Figures 4–8 also show that the ionic conductivity of PEAAs increased with the EO/K molar ratio decreasing with MPEGs of the same MWs in the whole temperature range. It is well known that the number of charge carriers plays an important role in ionic conductivity. With the concentration of K increasing, the number of charge carriers increased correspondingly, and this resulted in the improvement of the ionic conductivity.

To deeply understand the dependence of the conductivity on temperature, we treated the corresponding data with a linear fitting method. The relevant curves were divided into different linear parts, and each was in good agreement with the Arrhenius equation and showed the typical features of ionic conduction.[21,22] Figure 4 shows that, with the exception of S2-10, the conductivity of S2-*X* ($X = 6$ or 8) linearly changed with the temperature over the entire temperature range. In the case of S4-*X* ($X = 6$, 8, or 10), S2-10, S6-6, and S6-8, the curves could be divided into two separate linear parts (sections A and B), whereas the curves of the rest of the sample could be divided into three well-separated linear parts (sections A, B, and C). This may be explained by the fact that S6-10, S8-*X*, and S10-*X* ($X = 6$, 8, or 10) had crystallinity to some extent because of the regular arrangement of the MPEG side chains. A phase transition from a crystalline morphology to an amorphous morphology at the end of section C could happen with the temperature. In the case of section B, the conductivity of the PEAAs abruptly increased with temperature; therefore, the activation energy of this section was crucial to the conductivity enhancement. The dependence of the corresponding activation energy on the MW of MPEG is plotted in

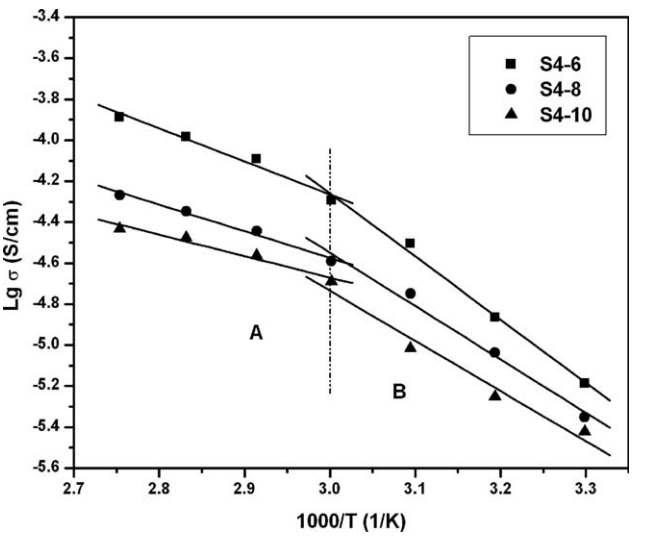

Figure 5 Dependence of the conductivity (σ) of S4-*X* ($X = 6$, 8, or 10) on temperature (T).

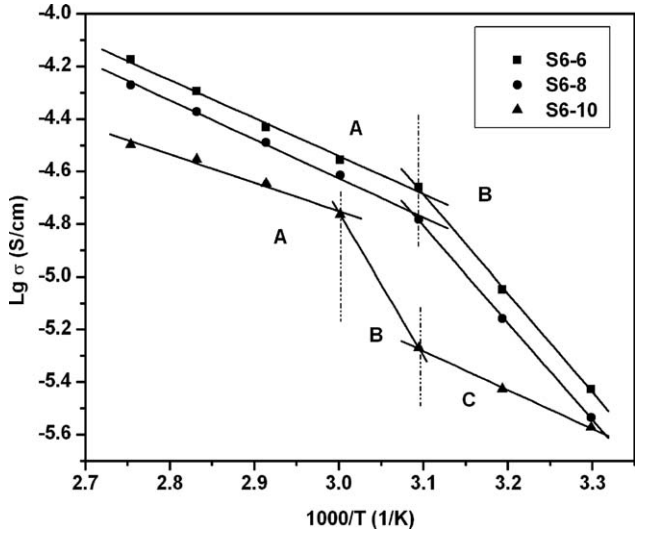

Figure 6 Dependence of the conductivity (σ) of S6-*X* (*X* = 6, 8, or 10) on temperature (T).

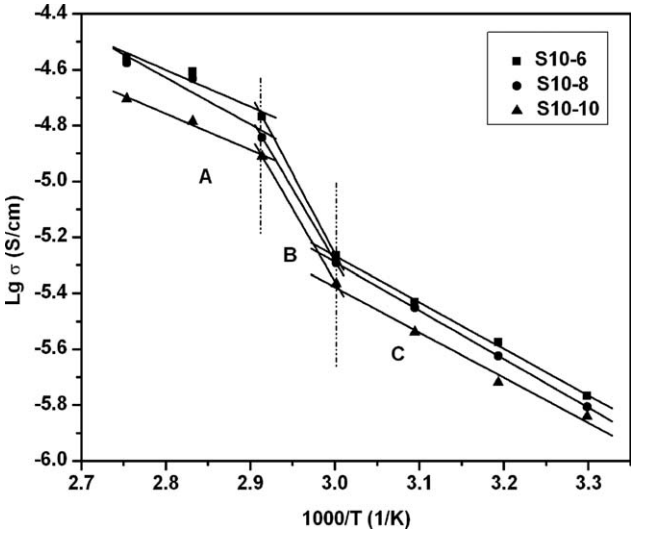

Figure 8 Dependence of the conductivity (σ) of S10-*X* (*X* = 6, 8, or 10) on temperature (T).

Figure 9. The average activation energy of the PEAAs linearly increased with the MW of MPEG; this indicated that MPEG of a higher MW (with more EO groups) resulted in lower conductivity. For section A, it seems that there were two mutually competitive factors:

1. The temperature actually increased both the concentration and migration of K.
2. It simultaneously enhanced the mobility of both the K and molecular segments,[20,23] and this led to the increase in the Coulomb repulsion between surrounding carriers and the decline of the free ion-conductive channels because they were probably occupied by the rearrangement of the flexible molecular segments.

However, the first factor was clearly dominant when both the carrier concentration and the temperature were not too high because the conductivity slightly increased with the temperature in this section.

Figures 10–12 demonstrate the dependence of the conductivity of the PEAAs on temperature with MPEGs of various MWs and with the same EO/K molar ratio. It is evident that, with some exceptions of crossing points in the high temperature region, the ionic conductivity of the PEAAs increased with the MW of MPEG decreasing when EO/K was constant. Moreover, it seems that the increasing crystallinity of the PEAAs adversely affected ion migration at a low temperature,[24] and a higher activation energy in section B also resulted in lower

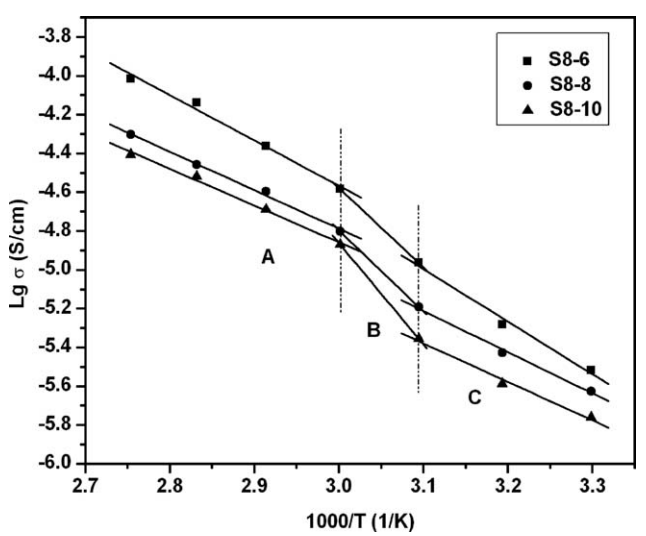

Figure 7 Dependence of the conductivity (σ) of S8-*X* (*X* = 6, 8, or 10) on temperature (T).

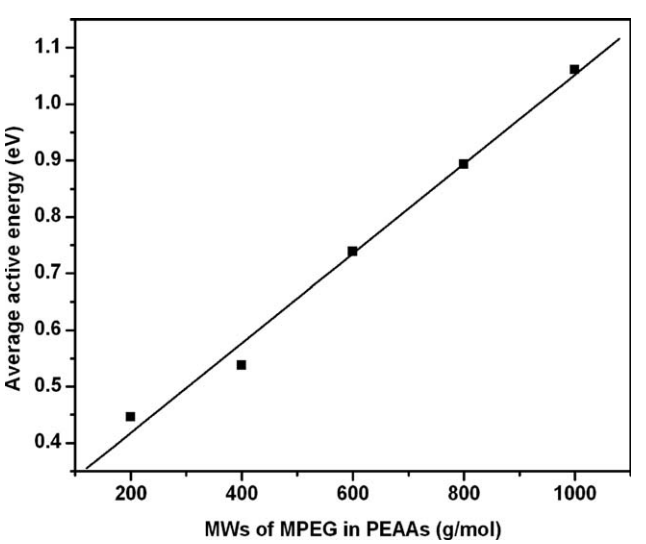

Figure 9 Effect of the MW of MPEG in PEAAs on the average activation energy in section B.

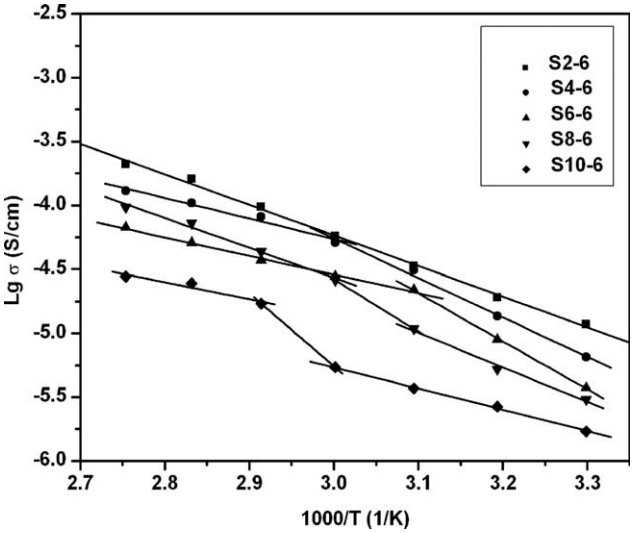

Figure 10 Dependence of the conductivity (σ) of SY-6 (Y = 2, 4, 6, 8, or 10) on temperature (T).

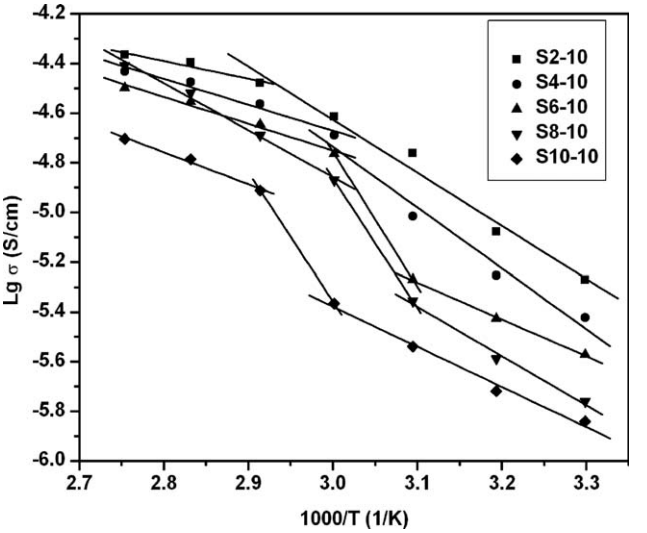

Figure 12 Dependence of the conductivity (σ) of SY-10 (Y = 2, 4, 6, 8, or 10) on temperature (T).

conductivity. The dependence of the conductivity of the PEAAs with the EO/K molar ratio of 6/1 on RH is displayed in Figure 13. The conductivity of the entire sample slightly decreased with RH decreasing, and it changed only within the same order of magnitude when RH decreased from 50 to 10%; this revealed the RH-insensitive capacity of the PEAAs. In addition, with the exception of S10-6, the RH of 30% seemed to be the critical value at which the conductivity of the samples changed abruptly. Moreover, the critical value gradually became unnoticeable with the MW of the MPEG branch increasing; this was attributed to the increasing crystallinity with MW. In the case of a sample with a higher crystallinity (e.g., S10-6), from a dynamic point of view, the relatively rigid molecular chains in the crystalline regions did not have enough energy to destroy the crystal lattices to rearrange the molecular chains and further coordinate with water molecules in the atmosphere. On the contrary, the flexible molecular chains of the amorphous sample could effectively coordinate with water molecules surrounded by hydrogen bonds.[11]

POM results

POM graphs of MPEGAs with different MWs and various types of PEAAs are shown in Figures 14(a–e) and 15(a–i), respectively. As shown in Figure 14(a,b), completely amorphous morphologies were detected for both MPEGA 200 and MPEGA 400

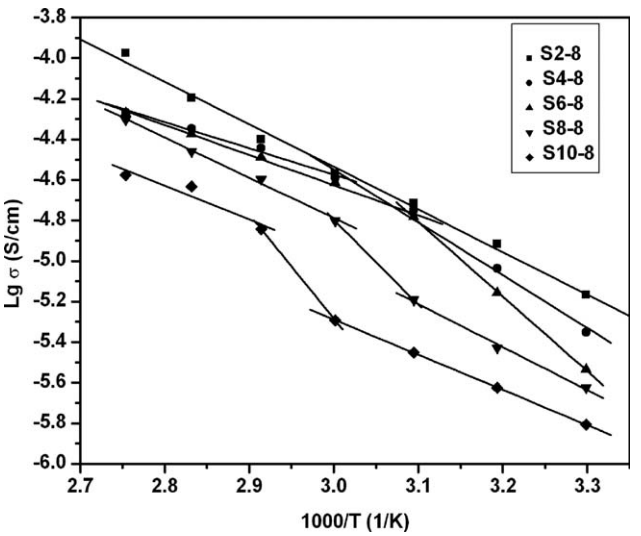

Figure 11 Dependence of the conductivity (σ) of SY-8 (Y = 2, 4, 6, 8, or 10) on temperature (T).

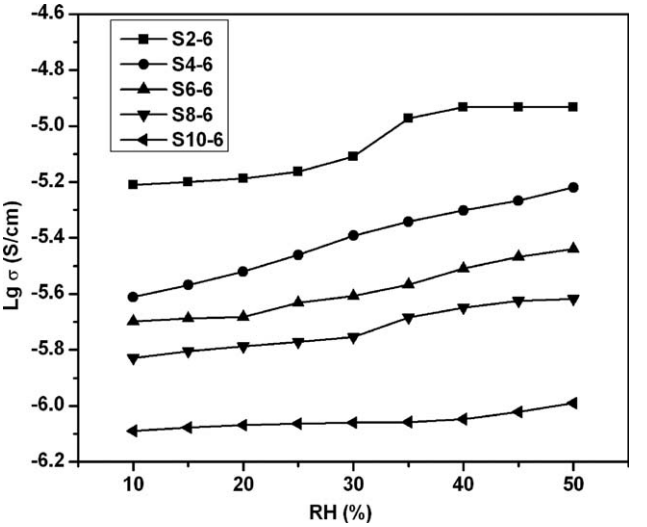

Figure 13 Dependence of the conductivity (σ) of SY-6 (Y = 2, 4, 6, 8, or 10) on RH.

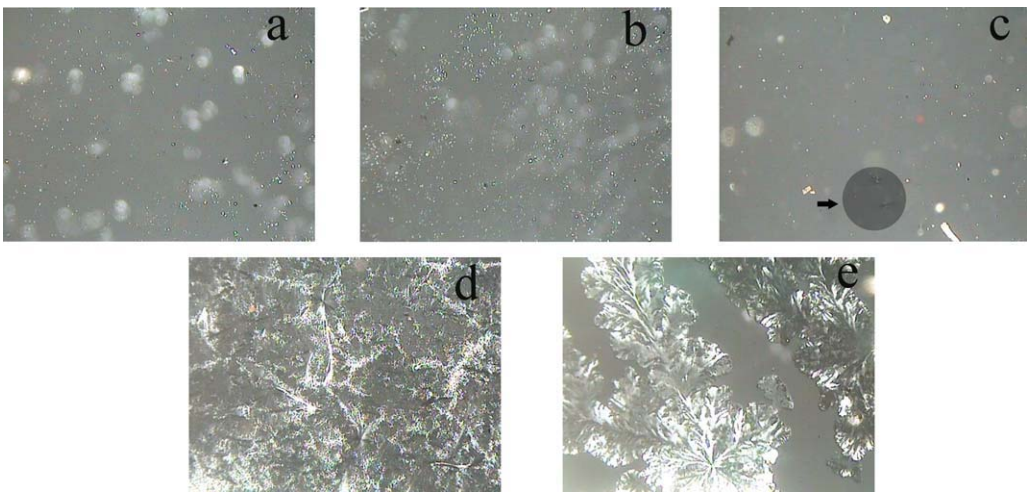

Figure 14 POM micrographs of MPEGA: (a) 200, (b) 400, (c) 600, (d) 800, and (e) 1000. [Color figure can be viewed in the online issue, which is available at wileyonlinelibrary.com.]

because no nucleation centers could be found. For the MPEGA samples with MWs of 600, 800, and 1000, more nucleation centers or spherulite crystals were seen with the MW increasing [Fig. 14(c–e)]. Different patterns of crystals were also observed with the MW. For the copolymers, the crystallization of the MPEGA side chains was partially suppressed by both copolymerization and an increasing salt concentration.[20,25] It is also clearly shown in Figure 15(a–i) that the crystallinity of the copolymers increased with the MW of MPEG at the same EO/K ratio because of the rise in the number of spherulite crystals. Both the crystallization and the crystal patterns correspondingly changed with the EO/K ratio with MPEGs of the same MWs. Therefore, from both conductivity and thermoprocessing points of view, a PEAA with an MPEG branch of the proper MW and a considerable EO/K ratio (e.g., S8-6) is indispensable for preparing corresponding PVC-based ESD packaging films; this takes into account the viscosity

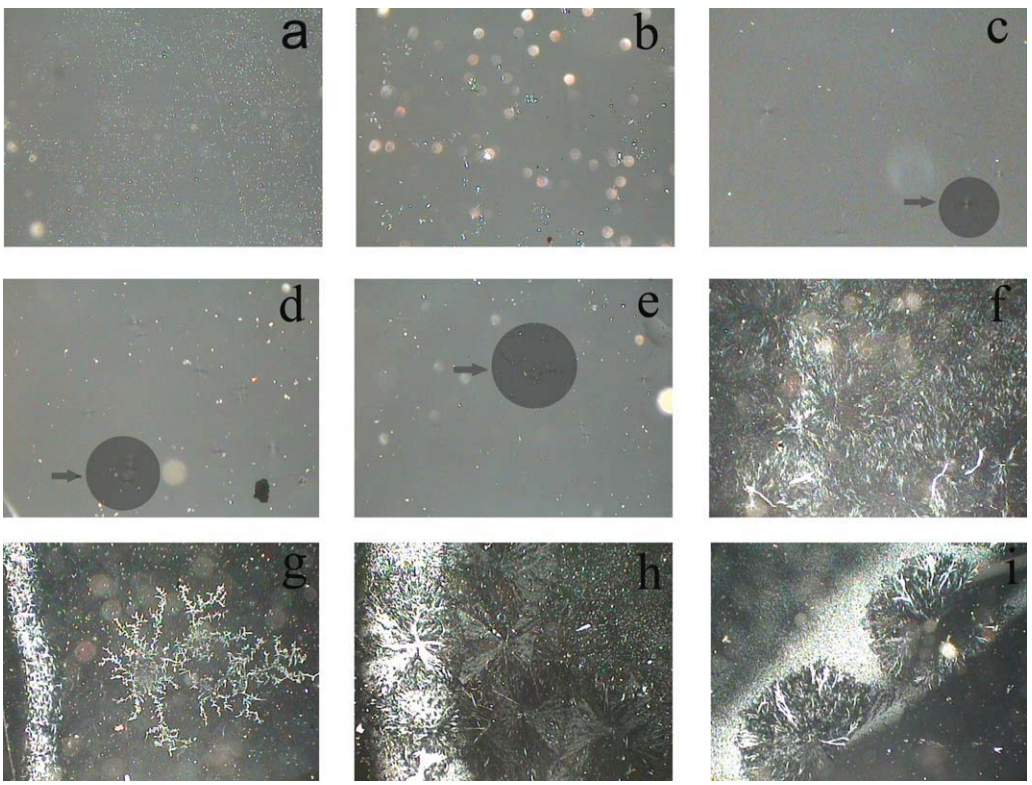

Figure 15 POM micrographs of (a) S6-6, (b) S6-8, (c) S6-10, (d) S8-6, (e) S8-8, (f) S8-10, (g) S10-6, (h) S10-8, and (i) S10-10. [Color figure can be viewed in the online issue, which is available at wileyonlinelibrary.com.]

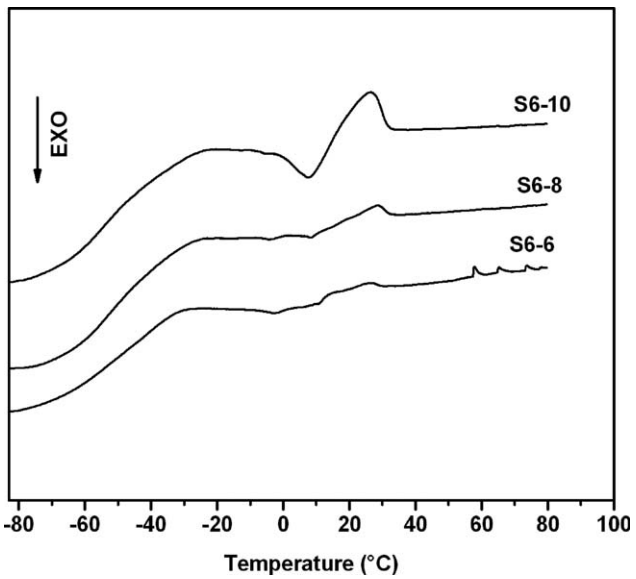

Figure 16 DSC thermographs of S6-*X* ($X = 6$, 8, or 10).

and dispersion of the PEAA at the processing temperature.

DSC analysis

DSC thermographs of S6-*X* ($X = 6$, 8, or 10) with different salt concentrations are shown in Figure 16. They reveal that the melting point of the sample almost appeared around 28°C, whereas the glass-transition temperature slightly increased from −52.2 to −48°C as the EO/K ratio decreased from 10/1 to 6/1. This was attributed to the fact that the K concentration increased with the EO/K ratio decreasing, and the number of transient crosslinking sites between K and EO of the MPEG side chain also increased correspondingly[26,27]; this partially interrupted the local motion of polymer segments. On the other hand, melting enthalpies of 0.2958, 0.7493, and 3.978 J/g were detected for S6-6, S6-8, and S6-10, respectively (Fig. 16). This illustrates that the crystallinity, calculated from the area of the melting peak, increased with the K concentration decreasing with the MPEG of the same MW and indicates that coordinated K prevented MPEG segments in PEAAs from crystallizing. It is well known that the ionic conductivity is closely proportional to the number of charge carriers and their mobility, and the number of charge carriers increases to some extent as the salt concentration increases. Therefore, the conductivity will be directly enhanced by the flexible motion of both EO groups and K for a low-crystallinity sample. On the contrary, the regular arrangement of polymer segments in crystalline regions usually restricts both the mobility of polymer chains and the diffusion of charge carriers, and this directly or indirectly leads to the reduction of the conductivity. The corresponding results are in good agreement with previous reports[24,25] and the analysis in the earlier section on conductivity measurements.

DSC thermographs of S*Y*-6 ($Y = 2$, 6, or 10) are shown in Figure 17. Sample S2-6 exhibited only a glass transition in the temperature range of −100 to 80°C, and no visible crystalline peak was detected. However, the glass-transition, cold-crystallization, and melting peaks of the crystal were found for both S6-6 and S10-6. The glass-transition temperatures for S2-6, S6-6, and S10-6 were −60, −48, and −34.5°C, respectively, and the crystallinity of the samples increased with the MPEG MW with the same EO/K ratio. The reason that the glass-transition temperature increased with the MPEG MW is that the length of the MPEG molecular chains increased with the MW; this implies that more polymer segments can be arranged into crystal lattices to crystallize. Therefore, the crystallinity of S*Y*-6 increased with the MPEG MW, whereas the mobility of both the polymer segments and K improved with the MPEG MW decreasing.

CONCLUSIONS

In this study, we successfully synthesized different types of PEAAs. The dependence of the ionic conductivity of the samples on the temperature followed the Arrhenius equation. The conductivity increased with the K concentration increasing with the same MPEG MW and also increased with the MW of MPEG decreasing when the EO/K molar ratio was constant. The study of the influence of the conductivity of PEAAs with MPEGs of different MWs at the same K concentration on the RH showed that the PEAAs synthesized here were

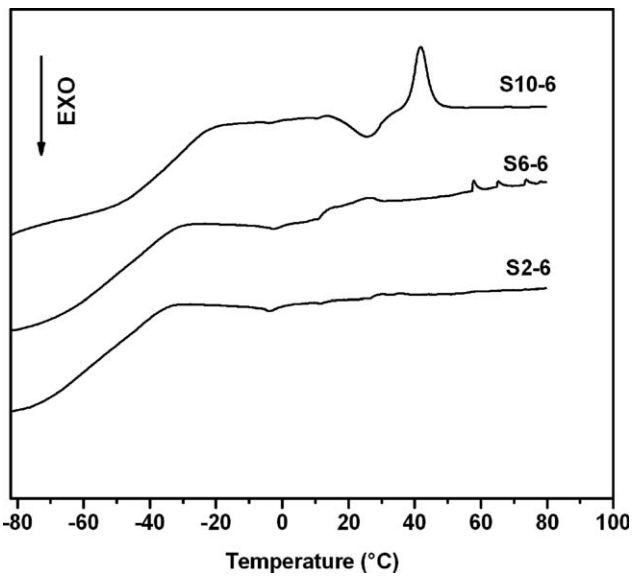

Figure 17 DSC thermographs of SY-6 ($Y = 2$, 6, 10).

almost insensitive to RH. The conductivity still reached 6.15×10^{-6} S/cm for S2-6 when the RH was 10%, and this indicated good potential for applications in the antistatic field. POM and DSC studies revealed that the conductivity was closely related to the crystallization of MPEG branches in PEAAs. The higher crystallinity of a sample usually restricted both the mobility of EO segments and the diffusion of K through crystallization and coordination effects and directly led to lower conductivity.

The PEAAs fabricated here have potential for the preparation of functional ESD packaging materials such as PVC- and PMMA-based ESD composites, especially when ESD protection at a low RH is needed.

References

1. Chen, G.; Wu, C.; Weng, W.; Wu, D.; Yan, W. Polymer 2003, 44, 1781.
2. Wang, G. Q.; Zeng, P. Polym Eng Sci 1997, 37, 96.
3. Novak, I.; Krupa, I.; Janigova, I. Carbon 2005, 43, 841.
4. Novak, I.; Krupa, I.; Chodak, I. Synth Met 2004, 144, 13.
5. Grob, M. C.; Minder, E. Plast Addit Compos 1999, 1, 20.
6. Monte, S. J. Polym Polym Compos 2002, 10, 1.
7. Ratner, M. A.; Shriver, D. F. Chem Rev 1988, 88, 109.
8. Murate, K. Electrochim Acta 1995, 40, 2177.
9. MacGlashan, G. S.; Andreev, Y. G.; Bruce, P. G. Nature 1999, 29, 792.
10. Bruce, P. G.; Campbell, S. A.; Mary, P. L. Solid State Ionics 1995, 78, 191.
11. Wang, J. L.; Yang, W. Q.; Lei, J. X. Polym Eng Sci 2009, 50, 57.
12. Wang, J. L.; Yang, W. Q.; Lei, J. X. J Electrostat 2008, 66, 627.
13. Yang, W. Q.; Wang, J. L.; Lei, J. X. Polym Eng Sci 2010, 50, 739.
14. Wang, J. L.; Yang, W. Q.; Tong, P. C.; Lei, J. X. J Appl Polym Sci 2009, 115, 1886.
15. Che, R. S.; Yang, W. Q.; Wang, J. L.; Lei, J. X. J Appl Polym Sci 2010, 116, 1718.
16. Hou, W. H.; Chen, C. Y. Electrochim Acta 2004, 49, 2105.
17. Hou, W. H.; Chen, C. Y.; Wang, C. C.; Huang, Y. H. Electrochim Acta 2003, 48, 679.
18. Digar, M.; Hung, S. L.; Wang, H. L.; Wen, T. C.; Gopalan, A. Polymer 2002, 43, 681.
19. Jannasch, P. Polymer 2001, 42, 8629.
20. Basak, P.; Manorama, S. V. Solid State Ionics 2004, 167, 113.
21. Reddy, M. J.; Chu, P. P. J Power Sources 2004, 135, 1.
22. Wang, M. K.; Zhao, F.; Dong, S. J. J Phys Chem B 2004, 108, 1365.
23. Tiyapiboonchaiya, C.; Pringle, J. M.; Sun, J. Z.; Byrne, N.; Howlett, P. C.; Macfarlane, D. R.; Forsyth, M. Nature 2004, 3, 29.
24. Marzantowicz, M.; Krok, F.; Dygas, J. R.; Florjanczyk, Z.; Monikowska, E. Z. Solid State Ionics 2008, 179, 1670.
25. Marzantowicz, M.; Dygas, J. R.; Krok, F.; Lasinska, K.; Florjanczyk, Z.; Monikowska, E. Z.; Affek, A. Electrochim Acta 2005, 50, 3969.
26. Xu, W.; Angell, C. A. Solid State Ionics 2002, 147, 295.
27. Hou, W. H.; Chen, C. Y.; Wang, C. C.; Huang, Y. H. Electrochim Acta 2003, 48, 679.